Water Practice & Technology

IWA PUBLISHING

Water Practice & Technology Vol 17 No 7, 1470 doi: 10.2166/wpt.2022.075

Characteristics of the water cycle of Jinan karst spring in northern China

Xing Deng[a], Liting Xing[a,b,*], Miao Yu[a,b], Zhenhua Zhao[c], Changsuo Li[c] and Qingwei Su[c]
[a] School of Water Conservancy and Environment, University of Jinan, 336 Nanxinzhuang West Road, Jinan 250022, China
[b] Shandong Engineering Technology Institute for Groundwater Numerical Simulation and Contamination Control, Jinan 250022, China
[c] Shandong Provincial Geo-mineral Engineering Exploration Institute, Jinan 250014, China
*Corresponding author. E-mail: stu_jnedu@126.com

ABSTRACT

Due to the multi-scale nature and complexity of the flow field, it has always been difficult for hydrogeologists to accurately grasp the water cycle characteristics of the karst water flow system. The inverse statistical model and IsoSource model were employed to calculate the spring age and the mixing ratio of spring recharge sources of the four large spring groups in Jinan. The karst hierarchical groundwater flow system was identified based on multiple factors. We found that the groundwater ages of Baotu Spring and Heihu Spring are about 6a–10a, and those of Wulongtan Spring and Pearl Spring are about 30a–35a. The main recharge sources of spring water of the four large spring groups were recognized as artificial recharge water, Ordovician karst water, and Cambrian Zhangxia Formation karst water. There were distinct differences in the recharge proportion of the four large spring groups. Three groundwater flow systems were identified according to multiple factors, which were local, intermediate, and regional. Furthermore, different levels of groundwater flow systems were recharged to the four large spring groups in different proportions. The research results provided new insights into the analysis of the hierarchical cycle and evolution of karst water.

Key words: groundwater flow system, ^{3}H age, Jinan spring domain, karst water, recharge source

HIGHLIGHTS

- The spring age of the four large spring groups is corrected by ISM model.
- The IsoSource model is used to calculate the mixing ratios of recharging water sources of the four large spring groups.
- Identify the karst hierarchical groundwater flow system in Jinan spring domain by combining multiple factors.

1. INTRODUCTION

Karst is widely distributed all over the world. Rich water resources could guarantee the development of our society. However, under the influence of human activities, the vulnerability of karst ecosystem is prominent. The sharp decrease of karst spring flow and the deterioration of water quality have become serious problems all over the world (Chu *et al.* 2017; Sun *et al.* 2017; Liang *et al.* 2018). The karst area in northern China is 992,000 km^2, which is distributed in 13 provinces (Liang & Zhao 2018) (districts and cities). In recent years, the karst ecological environment has also been plagued by many problems such as pollution and destruction (Xing *et al.* 2010; Yang *et al.* 2016). Over the years, great investment has been made in the restoration of famous springs in Shanxi (Yuan 2010; Wang *et al.* 2020), but the restoration effect is not significant. Taking Jinan as an example, to restore the continuous gushing of famous springs, a number of spring conservation measures have been taken successively, such as mining outside and supplementing inside, diverting the Yellow River from the reservoir to protect the spring, shutting down mining, and a surface water to groundwater artificial recharge project (Xing 2006; Hu *et al.* 2011; Xing *et al.* 2018). However, the threat of spring water cut-off in the dry season still cannot be eliminated. The fundamental reason is the lack of in-depth understanding of the cyclic evolution mechanism of different levels of flow system, and there is a certain blindness in formulating spring protection countermeasures.

The regional groundwater flow theory (Toth 1963) proposed by the hydrogeologist Toth describes the law of regional groundwater circulation better, and believes that the groundwater circulation does not completely depend on the geological structure, but is also controlled by the topographic potential energy (Liang *et al.* 2012, 2022). The local groundwater flow system has short runoff, shallow depth, large circulation depth, and

long retention time. Therefore, the hierarchical groundwater flow system has different hydrodynamic, physical and chemical characteristics and manifestations. Taking the groundwater flow system of Ordos Cretaceous Basin as an example, Jiang (2011) deduced the analytical solutions of water head and flow function on the two-dimensional section of the basin, and directly simulated the age distribution in the groundwater flow system by using the groundwater age control equation. Wang (2015) proposed three methods of geophysical prospecting, conductivity, and residence time to divide the level of flow system, established the 'late peak' method based on the retention time distribution of groundwater in the basin, and verified the effectiveness of this method, which has valuable reference significance for the study of the karst spring flow system. Wang (2016) revealed the relationship between karst hot water and regional groundwater flow in carbonate heat reservoir and the circulation characteristics of groundwater at different scales. Through the retention time and age distribution of groundwater, they identified the nested structure of multistage groundwater flow system in the basin, and reexamined the circulation and evolution process of groundwater from the perspective of time domain. Xiao *et al.* (2022) used numerical simulation and an indoor sandbox experiment to explore the interaction between seepage field and temperature field under different groundwater flow system development modes, and confirmed that temperature difference is an important driving force of a groundwater flow system in geothermal-rich areas. Gao *et al.* (2022) demonstrated the application of groundwater layered exploration technology in the study of a groundwater flow system, which laid a foundation for the determination of spatial movement direction of groundwater flow and the delimitation of groundwater flow system. In terms of practical application, Wang *et al.* (2021) used isotopes and hydrogeochemistry to reveal the groundwater flow pattern and recharge source in the aquifer system of arid inland basins in north-west China, and inferred the hydrogeochemical process in the process of groundwater circulation. Selene *et al.* (2020) studied the water rock interaction and mixing process of karst water system under the mining conditions of Mexico City, divided the groundwater flow system involved in mining into four parts, and confirmed the existence of water exchange among groundwater flow systems through reverse hydrogeochemical simulation. Hu *et al.* (2015) used hydrogen and oxygen stable isotopes to study the seasonal recharge of surface karst springs and the average residence time of surface karst water. Agoubi (2021) took the geothermal water resources in Tunisia as the research object, determined the heat source and flow pattern in different levels of groundwater flow system, and analyzed that the groundwater temperature and ion source in nonvolcanic areas depend on the retention time and circulation depth of groundwater.

The existing research results show that the regional groundwater flow system theory provides a theoretical basis for the division of a groundwater flow system and the in-depth exploration of the dynamic law of karst water. Only by correctly understanding and reasonably dividing the levels of groundwater flow system can we fully reveal the integrity, hierarchical structure, correlation, and systematic differences of karst springs, further excavate the unique hydrogeological information hidden in the recharge and discharge of spring water in Jinan and the common characteristics of karst springs in northern China. Although predecessors have studied the karst water system in Jinan, the lack of classification of the level of spring water flow system is not conducive to accurately depicting the dynamic changes of spring water, nor can it achieve the purpose of accurate spring conservation.

Therefore, in this study, the groundwater in Jinan spring karst aquifer is characterized by fixed depth stratified sampling monitoring, isotope and hydrochemical data, so as to more accurately characterize the characteristics of different levels of ground-water flow system. The purpose of this study is to explore the water cycle evolution model of karst water system, and correctly identify the hierarchical karst groundwater flow system combined with multiple factors, which can not only enrich the theory of karst water system, but also provide a theoretical basis for the protection of spring water in Jinan.

2. STUDY AREA

Jinan spring domain is located at 36 °40′N and 117° 00′E, the northern edge of the northern wing of Mount Tai uplift, with high terrain in the south and low terrain in the north. The overall spring domain extends to the Mashan fault in the west, surface watershed in the south, Dongwu fault in the east, and 500 m buried depth line of Ordovician limestone in the north (Qi *et al.* 2012). Yufu River, Beisha River, Xingji River, and other rivers are distributed. It belongs to a warm temperate continental monsoon climate, with annual average temperature of 14.7 °C and annual average precipitation of 671.1 mm, of which the rainfall from 2019a to 2021a is

683.5 mm, 736.0 mm, 1,089.7 mm. The stratum of Mount Tai Group (Art) in the spring area is the basement, and the overlying Paleozoic Cambrian and Ordovician strata are obliquely distributed from south to north, forming a monoclinal structure. From south to north, the metamorphic rocks, Cambrian and Ordovician limestones of Mount Tai Group are exposed in turn. The exposed Cambrian and Ordovician limestones in the south are easy to accept the infiltration of atmospheric precipitation, which is the main source of groundwater recharge in the spring area. The north is the Piedmont inclined plain covered by the quaternary system; there are intrusive magmatic rocks under it. The lithology of Cambrian stratum is mainly shale mixed with thin limestone, and the lithology of Ordovician stratum is mainly interbedded with limestone, dolomite, and calcareous shale (Meng 2021). Limestone karst pores, caves, dissolution fissures, and dissolution pipelines are developed, which provides a better storage space and migration path for groundwater (Sun & Peng 2014). Karst water generally moves from south to north. In the discharge area of the four spring groups, the limestone is covered by magmatic rocks with a thickness of more than 150 m, and has good pressure-bearing property. Blocked by magmatic rocks, it gushes out along the contact zone between limestone and magmatic rocks to form spring water. In addition, there are many NNW-trending faults in the spring area, breaking and collapsing aquifers and aquifers, connecting the hydraulic connection between Cambrian and Ordovician aquifers. Therefore, the karst water in the study area has the hydrogeological characteristics of homologous recharge, layered and directional runoff, horizontal conduction, and centralized discharge (Li 2021) (Figures 1 and 2).

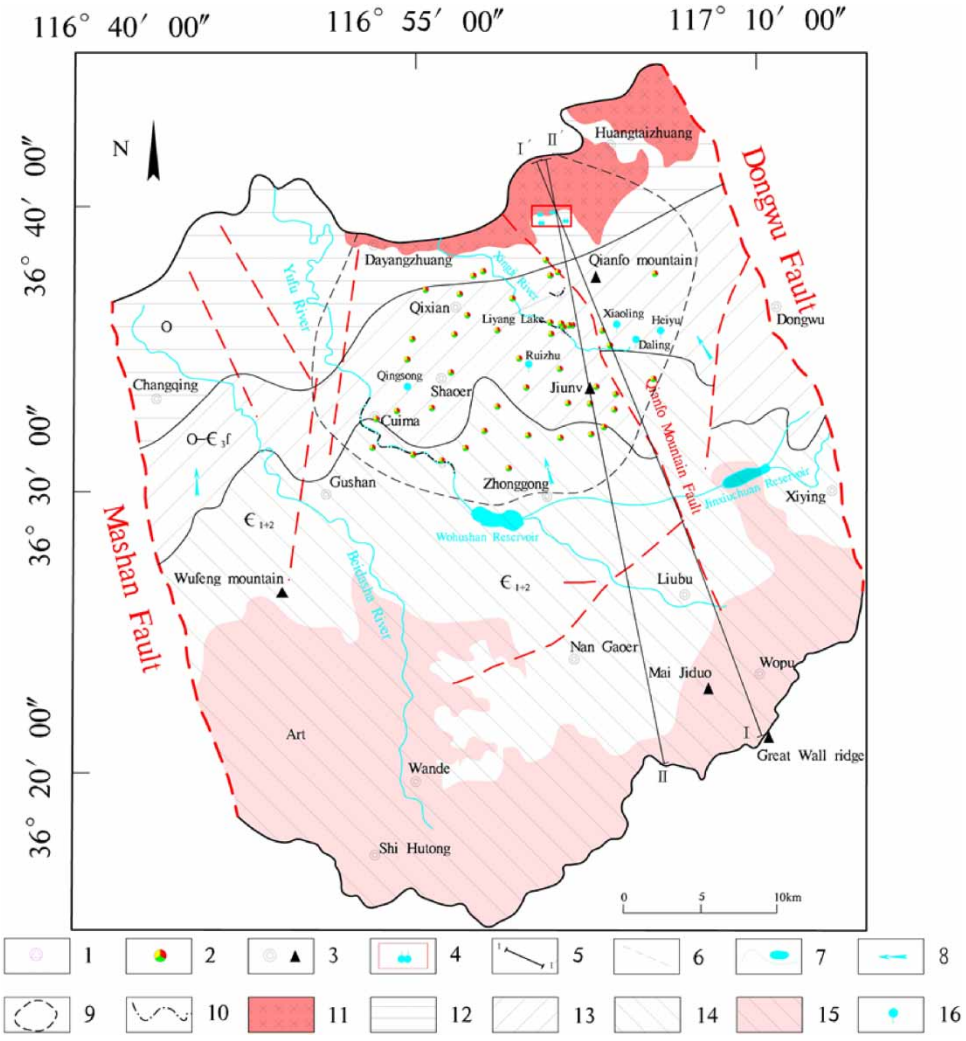

Figure 1 | Schematic diagram of Jinan spring domain in northern China. 1-surface water sampling point; 2-groundwater sampling point; 3-geographical location; 4-sampling point range of four large spring groups; 5-section line; 6-fault; 7-rivers and reservoirs; 8-flow direction of groundwater; 9-principal study area; 10-artificial recharge section; 11-intrusive rock; 12-runoff drainage area; 13-direct recharge area; 14-indirect recharge area; 15-archean metamorphic rocks; 16-seasonal spring.

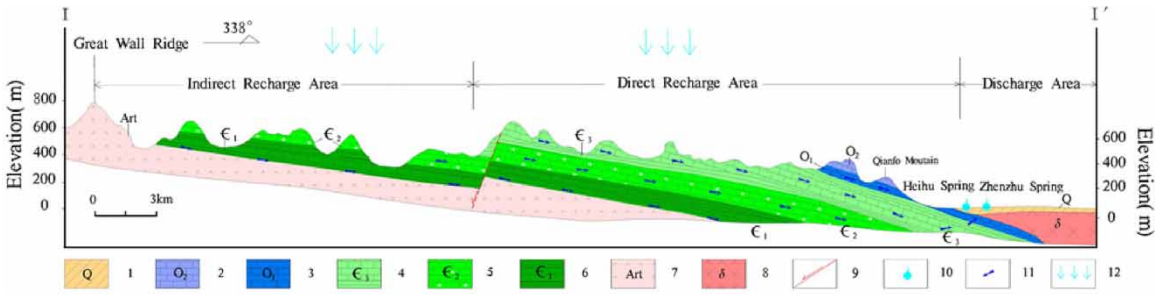

Figure 2 | Geological section of Jinan spring domain (I-I′). 1-Quaternary sediments; 2-Middle Ordovician; 3-Lower Ordovician; 4-Upper Cambrian; 5-Middle Cambrian; 6-Lower Cambrian; 7-Archean metamorphic rocks; 8-intrusive rock; 9-fault; 10-spring; 11-flow direction of groundwater; 12-precipitation.

3. METHODS

3.1. Sampling and analysis

A total of 71 sampling points were arranged in this study (Figure 1), including 3 recharge sampling points, 14 spring water sampling points, and 54 karst water sampling points of Cambrian and Ordovician limestone. Water samples were collected and stored in accordance with the operating procedures of the 'Standard Test Method for drinking water' (GB5750-2006). The conventional ion components are tested by hydrochemical titration and flame method. The test indexes include K^+, Na^+, Ca^{2+}, Mg^{2+}, HCO_3^-, SO_4^{2-}, Cl^-, and Sr^{2+} are detected by inductively coupled plasma emission spectrometer. Isotopic ^2H and ^{18}O ratios are detected by Xi'an Guolian Quality Detection Technology Co., Ltd with Picarro L2130-1 water isotope analyzer. The detection basis is BKR-FF-01-2016 'Determination of hydrogen and oxygen stable isotopes in water laser cavity ring down spectroscopy'. Isotopic ^3H samples were sent to the Institute of Hydrogeology and Environmental Geology, Chinese Academy of Geological Sciences for testing. Aqua TROLL 600 multiparameter water quality detector produced by In-Situ company was used to monitor the conductivity of spring and well water at fixed depth in real time in the field, and the conductivity resolution was 0.01 μS/cm, the monitoring frequency was 1–2 times per month, and the observation time was 2017a–2021a.

3.2. Tritium isotope dating

The highly heterogeneous and anisotropic development of karst aquifer media makes the law of groundwater migration extremely complex (Dong 2020), and there must be hydrodynamic dispersion (Liu *et al.* 2003). In this study, the inverse statistical model (Rose 1993) (ISM) is used to calculate the age of groundwater. Taking the dispersion parameters in the process of groundwater mixing as the standard deviation, the following algorithm can be used to calculate the average residence time range of groundwater level under different standard deviations.

The decay correction value of ^3H is calculated according to the annual tritium input data:

$$T_i' = T_i e^{-\lambda t} \tag{1}$$

T_i' is the tritium decay correction concentration in year i (TU); T_i is the tritium input concentration in a given year i (TU); λ is the decay constant, generally taken as 0.0558; t is the input year.

For the average decay corrected tritium value $(i, i+1)$ during the adjacent year (α), it is:

$$\alpha = \frac{T_i' + T_{i+1}'}{2} \tag{2}$$

The percentage weight of all mixed water is allocated to the average decay correction value during adjacent years, that is, each α value obtained from Equation (2).

Therefore, the weighted average tritium value year by year (M):

$$M = \alpha(A_{i,\ i+1}) \tag{3}$$

The total tritium concentration in the period with n-year data is the sum of each weighted average value in that period.

3.3. Hydrogen and oxygen stable isotope model

Hydrogen and oxygen isotopes are relatively stable and can be used as tracers to study the interaction between different water bodies (Sappa *et al.* 2012; Khalil *et al.* 2015). In this study, the IsoSource linear model (Phillips & Gregg 2003) is used to calculate the contribution rate of hydrogen and oxygen isotopes in different groundwater recharge sources to the concentration of hydrogen and oxygen isotopes in spring water.

Calculate all possible percentage combinations of resources according to the specified increment range:

$$M = \begin{pmatrix} (100/i) + (s-1) \\ s-1 \end{pmatrix} = \frac{[(100/i) + (s-1)]!}{(100/i)!(s-1)!} \tag{4}$$

M represents the number of combinations, i represents the increment range, and s represents the number of sources. The weighted average value of each combination is compared with the isotope value actually measured by the mixture to obtain a feasible solution. In all feasible solutions, the frequency of each resource contribution percentage is analyzed to obtain the contribution rate of different recharge sources.

The calculation process is executed by the Visual Basic program of IsoSource. All feasible source combinations can be obtained by providing the source of spring water recharge, the hydrogen and oxygen isotope values of the samples of the four large spring groups, as well as the required source increment and mass balance tolerance, and the IsoSource program can be downloaded and used on the official website of the U.S. Environmental Protection Agency (Phillips & Gregg 2003).

4. ANALYSIS OF CALCULATION RESULTS

4.1. The mean transit time of groundwater

According to the data of precipitation tritium concentration in Jinan spring area and formula (1) in this paper, the decay correction value of precipitation tritium concentration in Jinan spring area in each year is obtained (Table 1). Then calculate according to formulas (2) and (3). Based on the standard deviation of 5, 10, 15,…, 95, 100, the mean transit time of groundwater from 5a to 100a in Jinan spring domain is calculated (Table 2).

The test results indicated that the tritium concentrations of Baotu Spring, Heihu Spring, Tanxi Spring, and Wangfuchizi Spring were 8.5 TU, 6.9 TU, 8.6 TU, and 8.4 TU, respectively. Among them, the tritium concentration of Heihu Spring was significantly smaller than that of other springs. According to the water quality monitoring results (Table 3), the Cl^- concentration of the Heihu Spring group was greater than 70 mg/L, which was substantially larger than that of other spring groups by about 40 mg/L–60 mg/L. The ^3H concentration value was similar to that of domestic water, which was obviously smaller than that of atmospheric precipitation (Ren *et al.* 2000). We considered the Heihu Spring as a spring greatly affected by human activities, thus, the tritium concentration of the Heihu Spring was used as the basis for evaluating the age of spring water. Based on the calculation results of the ISM model, different tritium concentrations had three age distribution ranges: less than 10a, 30a–40a, and 50a–70a. Combined with the piston flow model and full mixing model (Yang 2008), the age distribution range of the four large spring groups was estimated to be 6a–35a. Combined with the hydrogeological conditions and genetic model of the four large spring groups in Jinan, the circulation depth of Baotu Spring and Heihu Spring was assessed to be less than that of Tanxi Spring and Wangfuchizi Spring (Sun *et al.* 2021). Moreover, the retention time of groundwater in the local groundwater flow system participating in the shallow cycle is considerably smaller than that in the regional groundwater flow system participating in the deep cycle (Jiang 2011). Thus, the spring age of Baotu Spring and Heihu Spring should also be less than that of Tanxi Spring and Wangfuchizi Spring (Fang *et al.* 1989; Zhang *et al.* 2012). Therefore, the groundwater age of Baotu Spring and Heihu Spring was corrected to 6a–10a, and the groundwater age of Tanxi Spring and Wangfuchizi Spring was corrected to 30a–35a. The age of groundwater is the embodiment of the difference between groundwater circulation and replacement rate, suggesting that the recharge sources and circulation depth of the four large spring groups are different.

Table 1 | Decay correction value of precipitation tritium concentration in Jinan spring domain from 1952a to 2020a

Year	Tritium concentration (TU)	Decay corrected concentration (TU)	Year	Tritium concentration (TU)	Decay corrected concentration (TU)	Year	Tritium concentration (TU)	Decay corrected concentration (TU)
1952	21.26	0.48	1975	84.21	6.84	1998	23.78	6.97
1953	27.68	0.66	1976	66.00	5.67	1999	16.01	4.96
1954	290.18	7.30	1977	81.30	7.38	2000	19.04	6.24
1955	42.66	1.13	1978	75.59	7.26	2001	18.94	6.56
1956	185.79	5.22	1979	61.40	6.23	2002	15.59	5.71
1957	119.72	3.56	1980	78.20	8.39	2003	14.29	5.53
1958	591.03	18.58	1981	68.50	7.77	2004	15.41	6.31
1959	454.82	15.12	1982	58.20	6.98	2005	15.42	6.68
1960	158.20	5.56	1983	42.80	5.43	2006	18.42	8.43
1961	229.69	8.54	1984	51.40	6.90	2007	15.06	7.29
1962	997.66	39.21	1985	46.80	6.64	2008	14.72	7.53
1963	2,876.60	119.55	1986	46.10	6.91	2009	14.77	8.00
1964	1,596.93	70.18	1987	43.00	6.82	2010	12.93	7.40
1965	722.54	33.57	1988	40.00	6.71	2011	14.04	8.50
1966	525.00	25.80	1989	36.00	6.38	2012	13.74	8.79
1967	299.06	15.54	1990	35.81	6.71	2013	13.89	9.40
1968	203.62	11.19	1991	39.54	7.84	2014	13.76	9.85
1969	247.54	14.38	1992	32.15	6.74	2015	11.89	8.99
1970	209.42	12.86	1993	24.40	5.41	2016	11.76	9.41
1971	230.00	14.94	1994	31.69	7.43	2017	11.00	9.30
1972	100.03	6.87	1995	33.91	8.40	2018	10.89	9.74
1973	89.00	6.46	1996	45.08	11.81	2019	11.26	10.65
1974	112.00	8.60	1997	31.05	8.60	2020	12.30	12.30

4.2. Calculation of spring water recharge source proportion by IsoSource model

Referring to the previous research results (Xing *et al.* 2018; Meng *et al.* 2020; Li *et al.* 2021), the spring water of the four large spring groups is the result of the combination of depth and depth and multi-source mixed recharge (Gao *et al.* 2014), and the spring water recharge sources are divided into (Figure 3) : artificial recharge water of Liyang Lake (1), artificial recharge water of Xingji River (2), Southeast Ordovician karst water (3), due south Ordovician karst water (4), southwest Ordovician karst water (5), Southeast Zhangxia Formation karst water (6), due south Zhangxia Formation karst water (7), karst water of Zhangxia Formation in the Southwest (8), artificial recharge water of Yufu River (9), karst water in Jixi (10).

According to the test results of ^{2}H and ^{18}O sampling analysis (Table 4), the percentage of spring water recharge sources in each division is calculated by using IsoSource linear model (Table 5). The calculation results of 10 recharge sources are summarized according to the type of water-bearing medium, recharge direction and recharge type, and the mixing ratio of spring water sources of four large spring groups is obtained (Table 6).

5. DISCUSSION

5.1. Identification of groundwater flow system elements

5.1.1. Identification of groundwater flow system based on groundwater level

Due to the different pressure-bearing properties of aquifers, the water level dynamics of different aquifers are also different. Therefore, the relationship between spring water level and each aquifer can be analyzed according to the water level dynamics of different aquifers. From south to north, from the karst water recharge area to the runoff discharge area of four spring groups, several karst water level dynamic monitoring points Z1, Z2, Z3, and Z4 are selected to qualitatively identify different levels of groundwater flow systems according to the

Table 2 | Calculated tritium concentration corresponding to different average residence time and standard deviation in Jinan area

	Standard deviation (years)																			
The mean transit time(a)	5	10	15	20	25	30	35	40	45	50	55	60	65	70	75	80	85	90	95	100
5	12	–	–	–	–	–	–	–	–	–	–	–	–	–	–	–	–	–	–	–
10	8	8	–	–	–	–	–	–	–	–	–	–	–	–	–	–	–	–	–	–
15	6	7	7	–	–	–	–	–	–	–	–	–	–	–	–	–	–	–	–	–
20	6	7	7	7	–	–	–	–	–	–	–	–	–	–	–	–	–	–	–	–
25	7	7	7	7	7	–	–	–	–	–	–	–	–	–	–	–	–	–	–	–
30	6	7	6	7	8	11	–	–	–	–	–	–	–	–	–	–	–	–	–	–
35	6	6	7	8	11	11	11	–	–	–	–	–	–	–	–	–	–	–	–	–
40	6	7	8	13	12	11	10	10	–	–	–	–	–	–	–	–	–	–	–	–
45	7	9	15	14	12	11	10	9	9	–	–	–	–	–	–	–	–	–	–	–
50	13	20	17	14	12	11	10	9	8	8	–	–	–	–	–	–	–	–	–	–
55	36	23	17	14	12	10	9	8	8	8	7	–	–	–	–	–	–	–	–	–
60	29	12	16	13	11	10	9	8	7	7	7	6	–	–	–	–	–	–	–	–
65	5	13	13	11	10	9	8	7	7	7	6	6	6	–	–	–	–	–	–	–
70	0	2	8	9	8	8	7	7	6	6	6	6	5	5	–	–	–	–	–	–
75	0	0	1	6	7	7	6	6	6	6	5	5	5	5	5	–	–	–	–	–
80	0	0	0	1	4	5	5	5	5	5	5	5	5	5	5	5	–	–	–	–
85	0	0	0	0	0	4	4	5	5	4	4	4	4	4	4	4	4	–	–	–
90	0	0	0	0	0	0	3	4	4	4	4	4	4	4	4	4	4	4	–	–
95	0	0	0	0	0	0	0	2	3	3	3	3	3	3	4	3	4	4	4	–
100	0	0	0	0	0	0	0	0	2	3	3	3	3	3	3	3	3	3	3	3

Note: The color represents the age distribution range of the four large spring groups calculated from the test data.

Table 3 | Ion content of spring water in four large spring groups

	Heihu Spring		Baotu Spring		Tanxi Spring		Wangfuchizi	
Ion content (mg/L)	2019a	2020a	2019a	2020a	2019a	2020a	2019a	2020a
K^+	1.18	0.85	1.2	1.67	2.27	2.42	–	1.02
Na^+	34.02	30.60	24.59	36.50	25.33	28.5	–	17.50
Ca^{2+}	130.26	137.00	120.84	111.00	106.81	111	–	114.00
Mg^{2+}	23.09	22.20	22	21.70	21.15	22.1	–	20.70
Cl^-	71.97	70.30	60.62	65.80	55.66	59.4	–	47.60
SO_4^{2-}	119.74	119.00	104.08	116.00	100.14	105	–	86.60
HCO_3^-	318.43	299.36	297.2	262.70	272.94	262.7	–	268.81

correlation between karst water level and Baotu Spring (Figure 4). Among them, Z1 water intake layer is Cambrian Zhangxia Formation aquifer, Z2 water intake layer is Ordovician Yeli and Liangjiashan Formation aquifer, Z3 water intake layer is Ordovician Yeli and Liangjiashan Formation, Z4 water in-take layer is Ordovician Yeli and Liangjiashan Formation, and Z3 and Z4 are 1.9 km and 1.5 km away from the four large spring groups respectively.

According to the correlation between different aquifers and Baotu Spring water level, the correlation between Zhangxia Formation aquifer water level and Baotu Spring water level in recharge area Z1 was poor, and R^2 was only 0.26. This indicated that the regional groundwater flow system participated in by the Zhangxia Formation aquifer had little contribution to Baotu Spring. The correlation between the water level of the aquifer of the Ordovician Yeli and Liangjiashan formations in the runoff area Z2 and the water level of Baotu Spring was general,

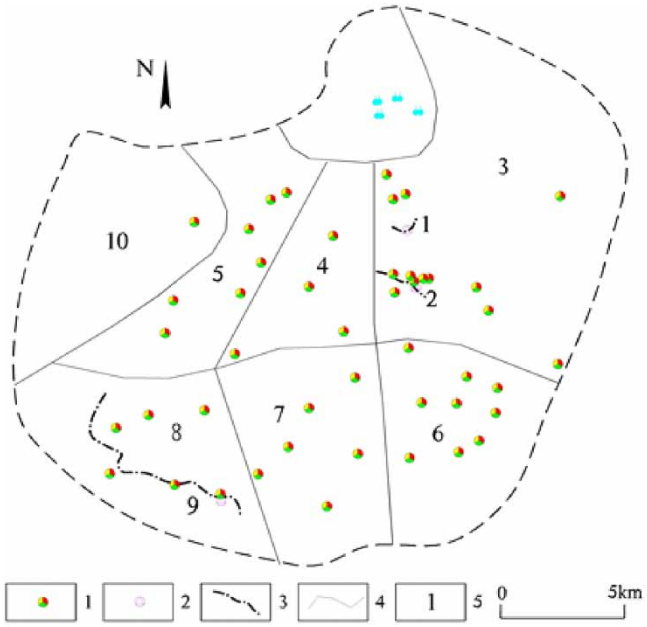

Figure 3 | Schematic diagram of recharge source calculation zoning. 1-groundwater sampling point; 2-surface water sampling point; 3-artificial recharge section; 4-zoning line; 5-Calculation number.

and R^2 was 0.63. Although the aquifers of Z3 and Z4 located in Jingshi Road and close to the four spring groups were the same, there was a great difference in correlation with the water level of Baotu Spring. Z3 had a good correlation with the water level of Baotu Spring, $R^2 = 0.84$, while Z4 had a poor correlation with the water level of Baotu Spring, $R^2 = 0.45$. Following the tracer tests at Z3 and Z4 (Chi 2019; Li 2021), the tracer injected by Z3 was not detected only in the Heihu Spring group, and different groundwater flow directions were identified according to the variation of tracer concentration at different depths. The tracer injected by Z4 was not detected in the four large spring groups. This demonstrates that there are multiple groundwater flow systems at different levels in the two places.

5.1.2. Identification of groundwater flow system based on stable hydrogen and oxygen isotope characteristics

The characteristics of hydrogen and oxygen isotopic composition of groundwater in different water-bearing horizons are different, and they show different recharge sources. According to the elevation effect of isotopes, the more negative the hydrogen and oxygen isotopic composition is, the higher the recharge elevation of groundwater is. Therefore, the grade of the water flow system can be divided according to the different hydrogen and oxygen isotopic composition range of groundwater (Wang 2016). The isotopic composition (^{18}O and ^{2}H) of spring water and borehole samples sampled in August 2020 is shown in Table 4. To characterize the isotopes of spring water samples and borehole samples in Jinan spring area, isotopic data are drawn in the isotopic δ^2H–$\delta^{18}O$ binary diagram of the sampling area (Figure 5). The equation describing the relationship between ^{18}O and ^{2}H of global atmospheric drawdown line (Craig 1961) (GMWL) and Jinan local atmospheric drawdown line (Liu *et al.* 2010) (LMWL) is as follows:

$$\text{GMWL, } \delta^2H = 8\delta^{18}O + 10 \quad (5)$$

$$\text{LMWL, } \delta^2H = 7.46\delta^{18}O + 0.90 \quad (6)$$

The main recharge source of groundwater in Jinan spring area is atmospheric precipitation, so each sampling point should be located near GMWL and LMWL. In the test results, the variation ranges of hydrogen and oxygen isotopic composition δ^2H and $\delta^{18}O$ of karst water are $-65.598‰ \sim -43.438‰$ and $-9.906‰ \sim -5.329‰$ respectively. The variation range of δ^2H and $\delta^{18}O$ is $-65.598‰ \sim -59.926‰$ and $-9.906‰ \sim -8.415‰$, and the variation range of conductivity is 500 μS/cm–1,022 μS/cm, this part of the sample points mainly come from the Cambrian Zhangxia Formation aquifer, so the runoff path is the longest and the hydrogen and oxygen isotopic composition is the most negative, which can be classified as supplied by the regional groundwater

Table 4 | δ^2H, $\delta^{18}O$ statistical table of sampling test results

Sampling number	Sampling time	$\delta^{18}O$	δ^2H	Sampling number	Sampling time	$\delta^{18}O$	δ^2H	Sampling number	Sampling time	$\delta^{18}O$	δ^2H
M1	2020/8	−6.62	−50.34	M25	2020/8	−8.04	−57.19	M49	2020/8	−9.02	−62.06
M2	2020/8	−6.51	−49.73	M26	2020/8	−8.53	−59.77	M50	2020/8	−8.69	−61.38
M3	2020/8	−8.10	−59.37	M27	2020/8	−7.96	−56.41	M51	2020/8	−8.77	−62.06
M4	2020/8	−8.34	−60.00	M28	2020/8	−7.93	−56.28	M52	2020/8	−8.97	−61.21
M5	2020/8	−8.08	−58.65	M29	2020/8	−8.57	−59.54	M53	2020/8	−9.43	−65.60
M6	2020/8	−8.10	−59.22	M30	2020/8	−8.87	−62.40	M54	2020/8	−9.91	−65.64
M7	2020/8	−8.23	−59.57	M31	2020/8	−8.69	−60.98	M55	2020/8	−8.22	−58.80
M8	2020/8	−7.88	−57.87	M32	2020/8	−5.80	−45.97	M56	2020/8	−7.51	−57.16
M9	2020/8	−8.03	−58.07	M33	2020/8	−8.48	−57.94	M57	2020/8	−8.08	−58.69
M10	2020/8	−7.86	−56.57	M34	2020/8	−6.34	−48.39	M58	2020/8	−7.67	−56.75
M11	2020/8	−8.28	−58.97	M35	2020/8	−6.77	−51.82	M59	2020/8	−8.07	−58.59
M12	2020/8	−7.40	−54.98	M36	2020/8	−5.33	−43.44	M60	2020/8	−7.91	−57.87
M13	2020/8	−7.60	−55.77	M37	2020/8	−8.73	−62.13	M61	2020/8	−8.08	−58.35
M14	2020/8	−8.81	−62.24	M38	2020/8	−8.42	−60.42	M62	2020/8	−8.00	−58.17
M15	2020/8	−8.15	−57.82	M39	2020/8	−8.63	−61.59	M63	2020/8	−7.69	−56.48
M16	2020/8	−8.09	−57.24	M40	2020/8	−8.33	−59.91	M64	2020/8	−8.12	−59.06
M17	2020/8	−8.39	−59.69	M41	2020/8	−8.43	−59.93	M65	2020/8	−8.10	−58.51
M18	2020/8	−8.35	−59.08	M42	2020/8	−8.71	−62.15	M66	2020/8	−7.97	−57.52
M19	2020/8	−8.67	−60.89	M43	2020/8	−8.44	−62.19	M67	2020/8	−7.84	−57.59
M20	2020/8	−8.22	−58.60	M44	2020/8	−8.22	−58.74	M68	2020/8	−7.91	−57.90
M21	2020/8	−8.19	−58.32	M45	2020/8	−8.21	−58.55	M69	2020/8	−7.42	−56.11
M22	2020/8	−7.64	−56.54	M46	2020/8	−8.80	−62.25	M70	2020/8	−7.57	−56.58
M23	2020/8	−8.07	−58.46	M47	2020/8	−8.89	−63.29	M71	2020/8	−7.60	−57.03
M24	2020/8	−7.99	−59.03	M48	2020/8	−8.88	−61.85				

Table 5 | Proportion of recharge

		Recharge ratio			
Recharge source		Baotu Spring	Heihu Spring	Wangfuchizi	Tanxi Spring
1	Artificial recharge water in Liyang Lake	14%	9%	14%	11%
2	Artificial recharge water in Xingji River	14%	12%	11%	11%
3	Artificial recharge water in Yufu River	14%	12%	11%	10%
4	Ordovician karst water in the southeast	6%	27%	8%	10%
5	Ordovician karst water due south	11%	18%	6%	11%
6	Ordovician karst water in the southwest	11%	9%	5%	13%
7	Karst water of Cambrian Zhangxia Formation in the southeast	6%	1%	17%	6%
8	Karst water of Cambrian Zhangxia Formation in due south	10%	2%	16%	8%
9	Karst water of Cambrian Zhangxia Formation in the southwest	5%	2%	3%	9%
10	Runoff karst water in the west of Jinan	10%	8%	10%	12%
Total		100%	100%	100%	100%

Table 6 | Mixing ratios of recharging water sources for the four largest spring groups

		Recharge ratio			
Recharge source		Baotu Spring group	Heihu Spring group	Pearl Spring group	Wulongtan Spring group
1	Artificial recharge water in Liyang Lake	14%	9%	14%	11%
2	Artificial recharge water in Xingji River	14%	12%	11%	11%
3	Artificial recharge water in Yufu River	14%	12%	11%	10%
4	Karst water in direct recharge area	28%	54%	19%	33%
5	Karst water in indirect recharge area	21%	5%	36%	23%
6	Runoff karst water in the west of Jinan	10%	8%	10%	12%
Total		100%	100%	100%	100%

flow system. The variation range of δ^2H and $\delta^{18}O$ is −51.824‰~ − 43.438‰ and −6.773‰~ − 5.329‰, the conductivity values are greater than 1,200 μS/cm, this part of the sample points are mainly taken from the aquifer of Majiagou Formation of Ordovician system, so the runoff path is the shortest, the hydrogen and oxygen isotope composition is the most positive, which is significantly affected by the atmospheric precipitation process, and can be classified as being replenished by the local groundwater flow system. Among them, four aquifer samples of Zhangxia Formation fall within the scope of the local groundwater flow system. The analysis shows that these four sampling points are only hundreds of meters away from the Yufu river that recharge the source, Due to the influence of recharge water, the isotopic composition is relatively positive. The variation range of δ^2H and $\delta^{18}O$ is −62.236‰~ − 54.975‰ and −8.807‰~ − 7.395‰, and the variation range of conductivity is 651 μS/cm–1,280 μS/cm. This part of the sample points is mainly from the aquifers of Ordovician Yeli and Liangjiashan Formation and Cambrian Fengshan Formation. Among them, the samples of 8 Majiagou Formation aquifers mixed with Yeli and Liangjiashan Formation aquifers fall within the area of intermediate groundwater flow system, indicating that the Majiagou Formation aquifer with positive hydrogen and oxygen isotopic composition and the relatively negative Yeli and Liangjiashan Formation aquifers have been mixed during drilling, perhaps the existence of faults leads to the mixing of water in the two aquifers. There is no significant difference in δ^2H and $\delta^{18}O$ between the aquifers of the Ordovician Yeli and Liangjiashan Formation and the underlying Cambrian Fengshan Formation. Therefore, it can be classified as being recharged by the intermediate groundwater flow system. It can be seen that the variation law of stable isotopes can indicate the recharge source of groundwater in the aquifer and the discharge characteristics of spring water, which is of indicative significance for the study of the water cycle and hydrodynamic characteristics of groundwater (Sappa *et al.* 2012).

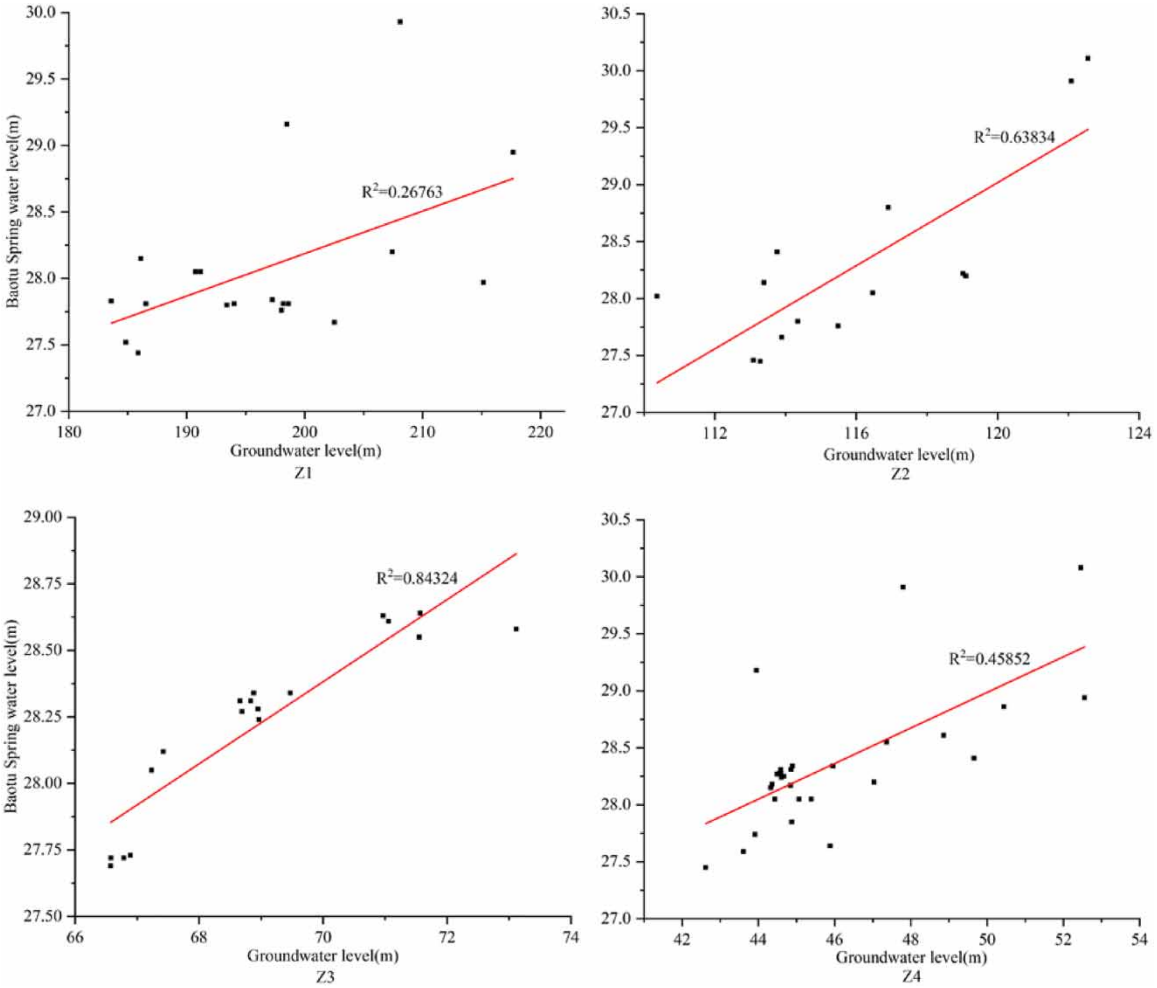

Figure 4 | Relationship between Baotu Spring and groundwater level.

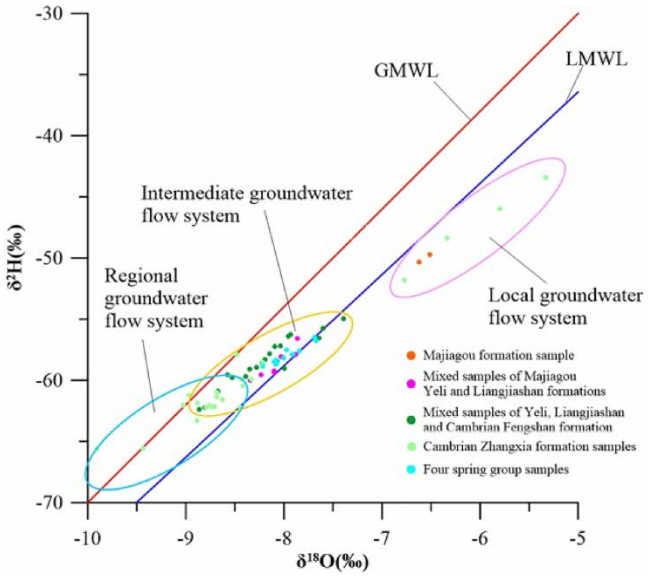

Figure 5 | Isotopes δ^2H–$\delta^{18}O$ binary graph.

5.1.3. Identification of groundwater flow system based on groundwater spillover zone

Groundwater spillover zones are usually exposed in the form of springs. Daily monitoring found that the form of downwelling spring below Xiaoling Spring near Xiaoling village appears with the infiltration and recharge of atmospheric precipitation in wet season. At the end of wet season, the spring flow gradually decreases until it dies out, belonging to a typical epikarst spring (Jiang & Yuan 1999). The epikarst spring system is a typical representative of the local groundwater flow system. Its recharge area is relatively small. It is mostly discharged to the surface in the form of seasonal karst springs, which has the characteristics of nearby infiltration recharge, runoff, and discharge (Liu 1991; Jiang & Guo 2009; Hu *et al.* 2015). Local groundwater flow system is affected by hierarchical nested mode and terrain, so it often shows the characteristics of small recharge range, short runoff path, and single discharge form. For example, Dongpo Spring group and Yinfang Spring in the core scenic spot of Huanglong, Sichuan, China (Liu *et al.* 2021). Through the test, the conductivity of Xiaoling Spring is 600 μS/cm, far less than the spring water conductivity of the four spring groups in the centralized discharge area 735 μS/cm–1,059 μS/cm, according to the stratigraphic structure near Xiaoling Spring, the genetic model of spring water is analyzed, as shown in Figure 6.

The surface lithology of the exposed position of Xiaoling Spring is a quaternary system, the underlying Ordovician stratum has been missed, and the surrounding mountains are exposed by the Cambrian Fengshan Formation. After precipitation infiltration, the head pressure of the Cambrian Fengshan Formation aquifer increases. Due to the relative water isolation of the underlying Cambrian Gushan and Changshan Formation, it discharges and flows in Xiaoling Spring and participates in the local groundwater flow system greatly affected by seasonal changes.

There is groundwater spillover in the Xingji river channel. The cause is that the mountains of the nearby Ordovician Majiagou Formation are supplied by atmospheric precipitation. The groundwater flows down the mountains under the action of gravity, and finally overflows in the Xingji river channel with relatively low terrain. The groundwater in the north mountain is discharged into the Xingji river channel to the south, and the overall groundwater flow direction is from south to north. It shows that this is the local groundwater flow system participated in by the Ordovician Majiagou Formation aquifer (Figure 7).

In addition, the weathering layer of Archaean metamorphic rocks, Cambrian Mantou Formation, Cambrian Zhangxia Formation, and Ordovician Yeli and Liangjiashan Formation aquifers in the southern mountainous area all have seasonal springs participating in the local groundwater flow system, such as Qingsong Spring, Daling Spring, Heiyu Spring, Ruizhu Spring, etc. The outflow time is from July to October with large rainfall, and the rest of the time is cut off. This shows that the local groundwater flow system is widely distributed and basically covers the whole Jinan spring domain under the influence of topography.

5.1.4. Identification of groundwater flow system based on the change of fixed depth conductivity

According to the borehole conductivity depth determination monitoring, the location of water-bearing fractures at different depths can be identified (Dhakate & Singh 2008), and the inflow velocity of single fracture in the well can be calculated through the conductivity peak of artesian well (Doughty *et al.* 2013). Due to the anisotropy of karst aquifer, groundwater seepage channel and other influencing factors, the variation characteristics of borehole conductivity with depth are obvious (Chi 2019). According to the characteristics of karst water recharge, runoff, and discharge in the spring area, the geological profile (Figure 8) and the fixed depth conductivity

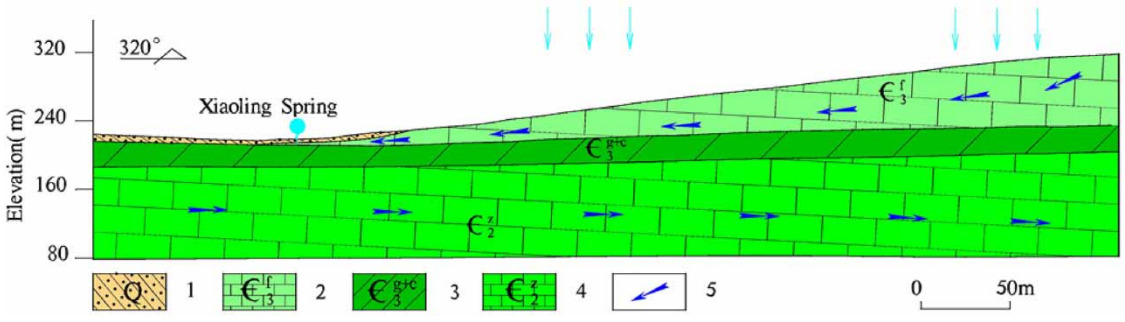

Figure 6 | Genetic profile of Xiaoling Spring. 1-quaternary system; 2-Cambrian Fengshan Formation limestone; 3-Cambrian Gushan Changshan Formation shale; 4-Cambrian Zhangxia Formation limestone; 5-flow direction of groundwater.

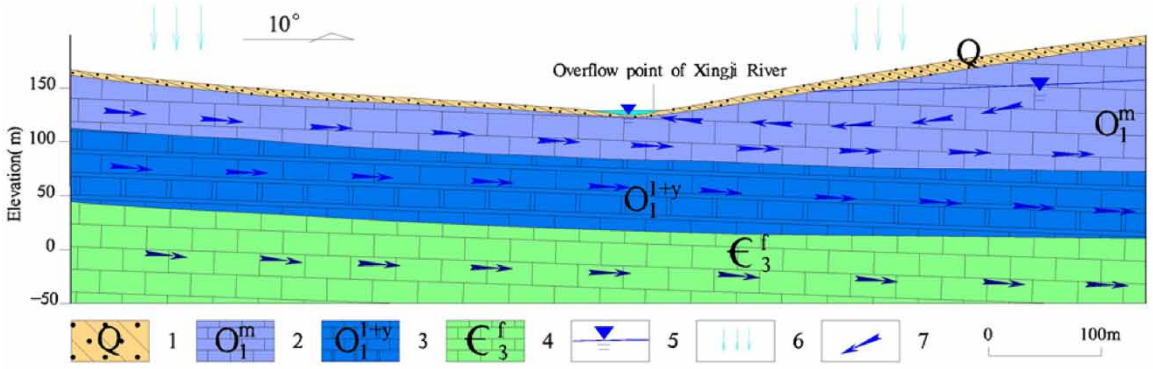

Figure 7 | Genetic profile Xingji River spillover. 1-quaternary system; 2-Ordovician Majiagou Formation limestone; 3-Ordovician Yeli Formation and Liangjiashan Formation limestone; 4-Cambrian Fengshan Formation limestone; 5-groundwater level; 6-atmospheric precipitation; 7-groundwater flow direction.

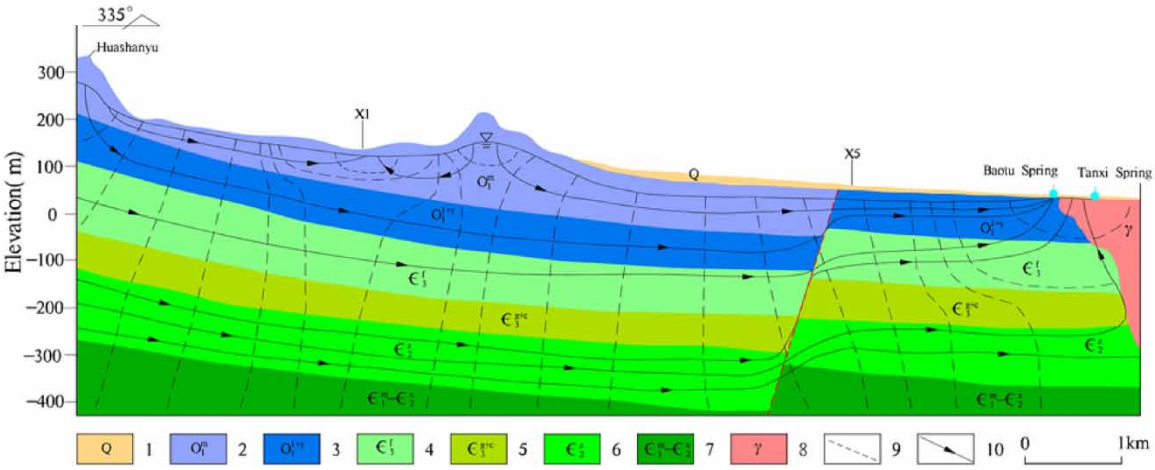

Figure 8 | Section from Huashanyu to Tanxi Spring. 1-quaternary system; 2-Ordovician Majiagou Formation; 3-Ordovician Yeli and Liangjiashan Formation; 4-Cambrian Fengshan Formation; 5-Cambrian Gushan and Changshan Formation; 6-Cambrian Zhangxia Formation; 7-Cambrian Mantou and Xuzhuang Formation; 8-intrusive rock; 9-equipotential line; 10-karst flow line.

curve of different boreholes (Figure 9) are selected to identify the different levels of groundwater flow systems involved in each aquifer.

Field observations showed that borehole X1 experienced artesian flow many times after heavy rainfall in August 2019 and July 2021. By analyzing the fixed depth conductivity value combined with the formation data, we found that the conductivity curve presented a 'three-stage' structure affected by three different groundwater flow systems (Figure 9(a)). Due to the different recharge sources and runoff paths of different groundwater flow systems, the conductivity of groundwater varied greatly. The analysis revealed that the artesian flow of the X1 borehole in 2019 and 2021 belonged to the artesian flow of different groundwater flow systems. Since August 10, 2019, the duration of heavy rainfall is three days. The statistical rainfall of the rainfall station nearest to the borehole was 323.8 mm. The conductivity test results after gravity flow manifested that the buried depth was 170 m, the shallow conductivity value was the fixed value of 860 μS/cm, and there was a sudden change in the conductivity value at the buried depth of 100 m–130 m. We inferred that there should be a large groundwater seepage channel here, which is discharged along the borehole under the influence of direct precipitation recharge. Since July 27, 2021, the duration of heavy rainfall is three days, and the rainfall is 116 mm. The conductivity test results after artesian flow suggested that the buried depth was 110 m, and the shallow conductivity value remained 585 μS/cm. The comprehensive analysis demonstrated that the conductivity value after gravity flow in 2019 was 860 μS/cm which was meaningfully bigger than the conductivity value of 585 μS/cm after gravity flow in 2021. The conductivity value in the depth of 170 m after the artesian flow was equal to that before the artesian flow, and the conductivity value in the depth of 170 m after the artesian flow was less different from that in the second section of the 'three-stage' structure. Therefore, we deduced that the artesian depth in 2019 was greater

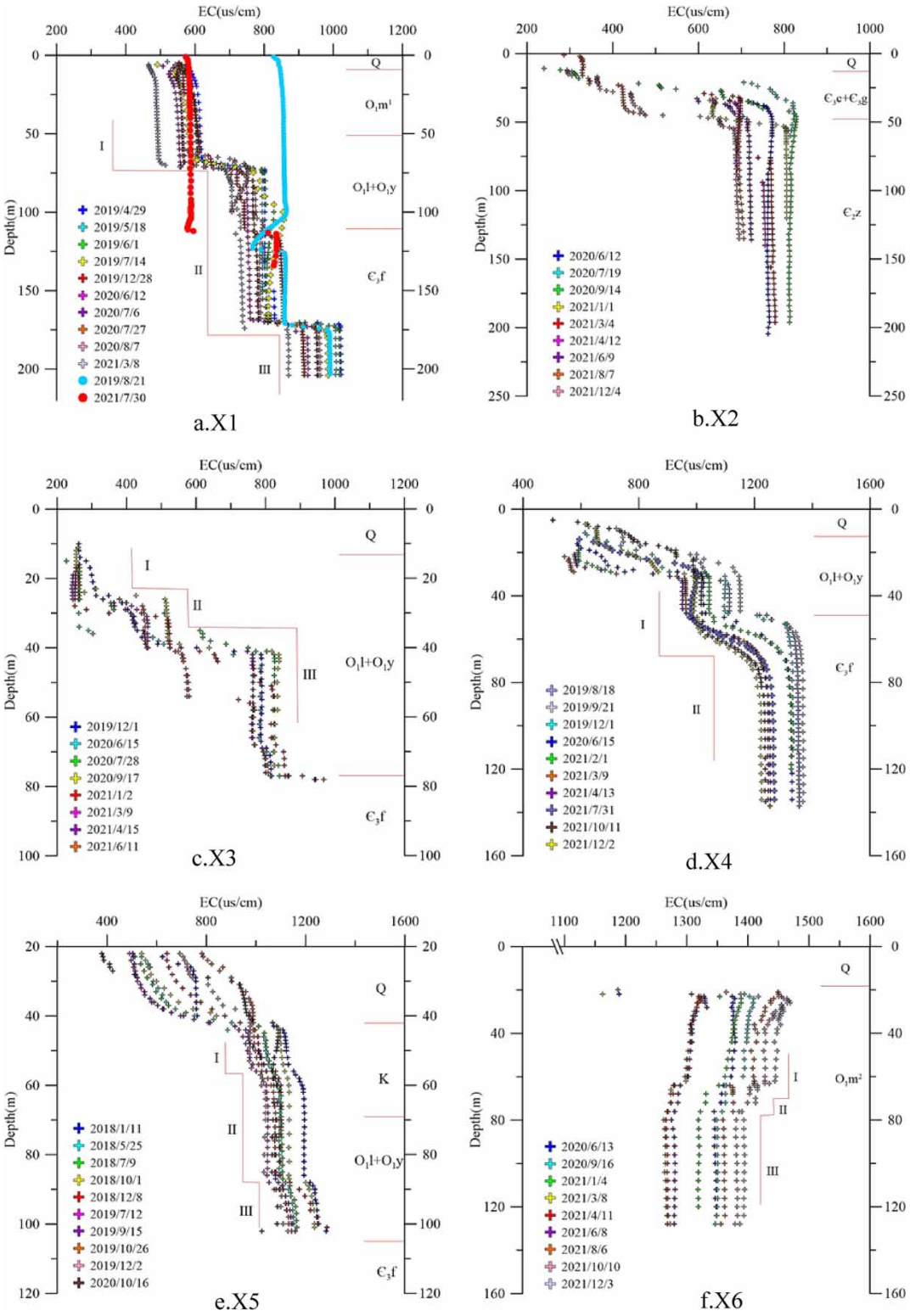

Figure 9 | Borehole fixed depth conductivity curve.

than that in 2021, belonging to the artesian flow of the intermediate groundwater flow system participated by the Fengshan Formation. The conductivity value after gravity flow in 2021 was 585 μS/cm, which was the same as the conductivity value of section I-I' in the 'three-stage' structure before artesian flow. Because of the influence of sealing and water stop during drilling, the fixed depth curve did not reflect the conductivity change of the local groundwater flow system participated by the Majiagou Formation. Therefore, the artesian flow in 2021

belonged to the confined artesian flow of the intermediate groundwater flow system participated by the Yeli and Liangjiashan formations. Artesian well is a typical hydrogeological phenomenon of groundwater circulation. Thus, studying the development mechanism and relevant characteristics of an artesian well can reveal the hydrodynamic characteristics of the groundwater flow system and can provide a reference basis for the identification of a multistage groundwater flow system (Hou *et al.* 2008; Wang 2015).

Boreholes X1, X2, X3, and X4 were located in the direct recharge area of the spring area, and boreholes X5 and X6 were located in the runoff discharge area. By comparing the conductivity values of boreholes, we found that although the water intake sections of boreholes X1 and X5 were Ordovician Yeli and Liangjiashan formation aquifers, the conductivity of X5 was about 600 μS/cm greater than that of X1. Combined with the geological profile, the groundwater runoff recharge path of borehole X1 was much smaller than that of borehole X5, so the conductivity value was too large. The shallow Ordovician Majiagou Formation aquifer has a high degree of karst development, small groundwater circulation depth, and fast flow velocity. Therefore, the conductivity value of borehole X6 was large, and the conductivity value was 1,300 μS/cm–1,400 μS/cm.

To sum up, according to the conductivity value of groundwater in different aquifers, combined with the length of groundwater runoff path and the influence of karst development degree, it can be identified that the Ordovician Majiagou Formation is mainly involved in the local groundwater flow system, the Ordovician Yeli, Liangjiashan Formation and Cambrian Fengshan Formation are mainly involved in the intermediate groundwater flow system, and the Cambrian Zhangxia Formation is mainly involved in the regional groundwater flow system, and the groundwater flow system at all levels is affected by the development degree of karst at different depths, and many sub-flow systems are developed.

5.1.5. Identification of groundwater flow system based on ion ratio relationship

When groundwater flows through carbonate rocks, minerals containing strontium and calcium dissolve synchronously, and the concentrations of Sr^{2+} and Ca^{2+} increase at the same time, but the solubility of strontium is less than that of calcium and its chemical properties are relatively stable, which makes $[Sr^{2+}]/[Ca^{2+}]$ better reflect the formation and runoff conditions of karst water. According to the dissolution degree of Strontium in aqueous media, the alternating intensity of water cycle in the karst water system can be judged (Guo & Wang 2006). According to the sampling test results, the relationship between $[Sr^{2+}]/[Ca^{2+}]$ value and TDS at each sampling point is obtained (Figure 10).

The study area can be divided into two areas. Region I is mainly the recharge runoff area, which is recharged by atmospheric precipitation. The alternating intensity of groundwater circulation is large and the runoff path is short, resulting in a short time of water rock interaction, making $[Sr^{2+}]/[Ca^{2+}]$ small, and TDS increase gradually with the runoff path. Region II is mainly the runoff and discharge area of spring groups. The runoff path of karst water from the exposed limestone area to the discharge area is long, the water rock interaction time is long, the Sr^{2+} concentration is large, and there is a large $[Sr^{2+}]/[Ca^{2+}]$. The $[Sr^{2+}]/[Ca^{2+}]$ in the sampling and test results of the four large spring groups are greater than 0.0025, distributed between 0.0025 and 0.00425. The distribution ranges of $[Sr^{2+}]/[Ca^{2+}]$ of the Zhenzhu Spring group, Wulongtan Spring group, and Baotu Spring group are slightly different, which are 0.0035–0.0040, 0.0032–0.0041 and 0.0036–0.0039 respectively, while the $[Sr^{2+}]/[Ca^{2+}]$ of Heihu Spring group is significantly smaller, which is 0.0026–0.0031, indicating that the four large spring groups are supplied by different groundwater flow systems and different runoff paths. Combined with the analysis of tritium isotope dating and the calculation results of the mixing ratio of stable isotope recharge sources, the age of Tanxi Spring and Wangfuchizi is 30a–35a. The karst water of the Cambrian Zhangxia Formation, which is mainly involved in the regional groundwater flow system, has the largest recharge proportion to the Zhenzhu Spring group, with a recharge proportion of 36%, followed by Wulongtan Spring group, with a recharge proportion of 23%. Therefore, the average residence time of Wangfuchizi is greater than Tanxi Spring. The age of Baotu Spring and Heihu Spring is 6a–10a. The recharge proportion of karst water from Ordovician Yeli Formation, Liangjiashan Formation and Cambrian Fengshan Formation, which mainly participate in the local groundwater flow system and intermediate groundwater flow system, to Baotu Spring group and Heihu Spring group is 28 and 54% respectively. Therefore, the horizontal residence time of Baotu Spring is greater than Heihu Spring. To sum up, Pearl Spring group and Wulongtan Spring group are replenished by the regional groundwater flow system with a long runoff path, and the spring water circulation renewal rate is slow, while Baotu Spring group and Heihu Spring group are replenished by the intermediate groundwater flow system and

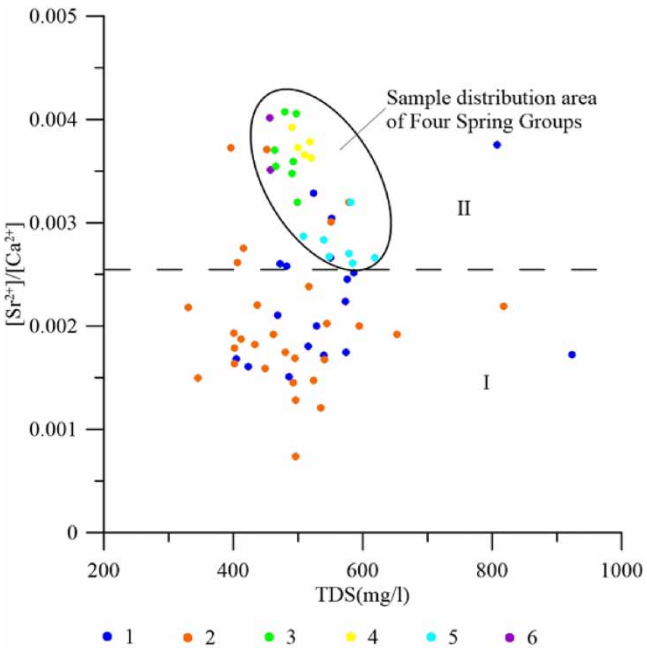

Figure 10 | Relationship Between $[Sr^{2+}]/[Ca^{2+}]$ Value and TDS. 1- samples of Ordovician and Cambrian Fengshan Formation; 2- samples of cambrian Zhangxia Formation; 3- samples of Wulongtan Spring group; 4- samples of Baotu Spring group; 5- samples of Heihu Spring group; 6- samples of Pearl Spring group.

local groundwater flow system with relatively short runoff path, and the spring water circulation renewal rate is fast.

5.2. Division of the multistage groundwater flow system in the spring domain

5.2.1. Classification of the groundwater flow system in the spring domain

The metamorphic rocks of the Neoarchean Mount Tai Group in the spring domain have large thicknesses and low fracture development. For this reason, it is difficult to form deep underground runoff. Usually, seasonal fissure springs with a small flow are formed, which converge to the valley rivers with the surface base flow and participate in the local groundwater flow system. The aquifer of Cambrian Mantou and Xuzhuang formations has general karst development and limited water storage space, so it is hard to form deep runoff. It is usually discharged into springs in the valley. This aquifer group that supplies the Zhangxia Formation aquifer locally is affected by structural faults and has little contribution to the four spring groups. Hence, this aquifer is also mainly involved in the local groundwater flow system. The recharge elevation of the Cambrian Zhangxia Formation aquifer in the indirect recharge area of four large spring groups is higher than that in the direct recharge area (Wang 2016). The surface karst and deep fractures are developed well. They receive the recharge of atmospheric precipitation to form underground runoff and then migrate to the deep. Some of them recharge the Ordovician aquifer of the Cambrian Fengshan Formation through faults and participate in the intermediate groundwater flow system. Furthermore, some of them expose to springs that are in the contact fracture zone of igneous rocks and participate in the regional groundwater flow system. The remaining migrate to the deep underground under the action of gravity to replenish the groundwater north of the Yellow River (Li 2021).

The comprehensive analysis shows that the Cambrian Zhangxia Formation aquifer in the study area mainly participates in the regional groundwater flow system. The Cambrian Fengshan Formation and Yeli and Liangjiashan Formation aquifers are mainly involved in the intermediate groundwater flow system. In the area with deep fissures, the groundwater will also carry out deep circulation under the action of gravity and participate in the regional groundwater flow system. The aquifer of the Ordovician Majiagou Formation mainly participates in the local groundwater flow system with shallow burial. In the fracture development area, there is a recharge effect of gravity on the aquifers of the Yeli, Liangjiashan Cambrian, and Fengshan Formation and participates in the intermediate groundwater flow system. Affected by the terrain, the Cambrian Zhangxia and Fengshan

Formation, Ordovician Yeli and Liangjiashan Formation may participate in the local groundwater flow system and are mostly discharged in the form of descending springs.

To sum up, section II-II' (Figure 11) has been selected along the direction of groundwater flow to divide the multistage groundwater flow system in Jinan spring domain.

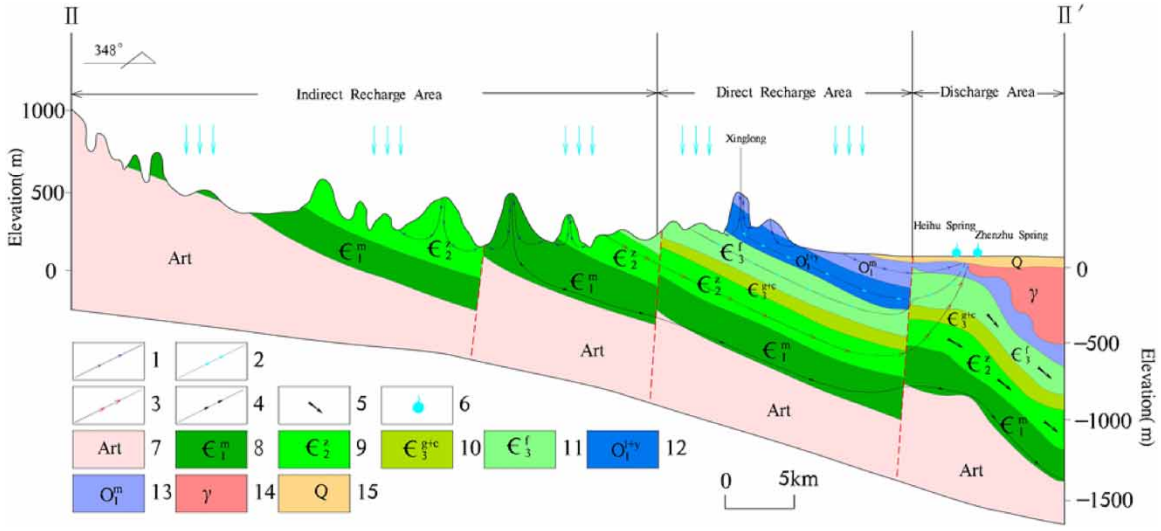

Figure 11 | Hierarchical groundwater flow system in Jinan spring domain. 1-local groundwater flow system; 2-intermediate groundwater flow system; 3-regional groundwater flow system; 4-archean surface fracture zone-groundwater flow of Mantou Formation; 5-flow direction of groundwater; 6-spring; 7-archean metamorphic rock; 8-Cambrian Mantou Formation; 9-Cambrian Zhangxia Formation; 10-Cambrian Gushan and Changshan Formation; 11-Cambrian Fengshan Formation; 12-Ordovician Yeli and Liangjiashan Formation; 13-Ordovician Majiagou Formation; 14-intrusive rock; 15-quaternary sediments.

5.2.2. Mixing ratios of recharging water sources for the four largest springs

The contents of δ^2H and $\delta^{18}O$ in the four large spring groups are different, indicating that the four spring groups receive mixed recharge from hierarchical groundwater flow systems participated in by different aquifers of Ordovician and Cambrian at the same time, and the recharge proportion is different. The calculation results of IsoSource model show that the aquifer of Ordovician Cambrian Fengshan Formation, which mainly participates in the local and intermediate groundwater flow system, accounts for the largest proportion of recharge to the four large spring groups, and Heihu Spring group > Wulongtan Spring group > Baotu Spring group > Pearl Spring group, accounting for 54, 33, 28, and 19% respectively. The Cambrian Zhangxia Formation aquifer, which is mainly involved in the regional groundwater flow system, accounts for a relatively small proportion of the recharge to the four large spring groups, and the recharge proportion of Pearl Spring group > Wulongtan Spring group > Baotu Spring group > Heihu Spring group accounts for 36, 23, 21, and 5% respectively. In addition, the recharge proportion of artificial reinjection water to the four large spring groups is also large, and the recharge proportion of Baotu Spring group > Pearl Spring group > Heihu Spring group > Wulongtan Spring group accounts for 42, 36, 33, and 32% respectively. The direct recharge area of spring water of the four large spring groups is the main recharge area of local groundwater flow system and intermediate groundwater flow system. Therefore, from the perspective of spring protection, under the condition of protecting the direct recharge area of spring water, the strata of Ordovician and Cambrian Fengshan Formation should be the best choice for artificial recharge.

It should be noted that the cyclic evolution of groundwater is an extremely complex hydrogeological process, and the recharge and mixing of groundwater in different periods are different. The recharge and mixing ratio of the multistage groundwater flow system to the four large spring groups were calculated by the samples taken in this study only to represent the static value at a certain time.

6. CONCLUSION

(1) According to the ISM model, the groundwater ages of Baotu Spring and Heihu Spring are 6a–10a, and the groundwater ages of Tanxi Spring and Wangfuchizi are 30a–35a. ISM model fully considers the

hydrodynamic dispersion of groundwater in a karst aquifer medium, and the calculation is simpler. Combined with hydrogeological conditions and traditional isotope mathematical model, a more accurate groundwater age distribution range can be obtained. Therefore, ISM model can be used as a basic method to determine the age of groundwater.

(2) Through the identification of the correlation between the groundwater level and the water level of Baotu Spring, the characteristics of hydrogen and oxygen isotopes of groundwater, groundwater spillover zone, artesian well, fixed depth conductivity curve, ion concentration ratio, and other factors, it is considered that the recharge proportion of the four large spring groups by different levels of groundwater flow system is different. The local groundwater flow system and intermediate groundwater flow system mainly participated by the aquifers of the Ordovician and Cambrian Fengshan Formation replenish the Heihu Spring group and Wulongtan Spring group in a large proportion, accounting for 54 and 33% respectively, and the Baotu Spring group and Pearl Spring group in a relatively small proportion, accounting for 28 and 19% respectively. The regional groundwater flow system mainly participated in by the Cambrian Zhangxia Formation aquifer has a large recharge proportion to the Pearl Spring group and Wulongtan Spring group, accounting for 36 and 23% respectively, and a relatively small recharge proportion to the Baotu Spring group and Heihu Spring group, accounting for 21 and 5% respectively.

(3) In the karst water system of the Jinan monoclinal structure, the hierarchical groundwater flow system is divided according to different aquifer structures. The shallow Ordovician Majiagou Formation aquifer is mainly involved in the local groundwater flow system, the Ordovician Yeli, Liangjiashan Formation aquifer and Cambrian Fengshan Formation aquifer are mainly involved in the intermediate groundwater flow system, and the Cambrian Zhangxia Formation aquifer is mainly involved in the regional groundwater flow system, which is affected by the terrain, each aquifer may participate in the local groundwater flow system. Among them, the Cambrian Fengshan Formation Ordovician aquifer participates in the intermediate groundwater flow system with the most complex characteristics and the largest contribution rate to the four large spring groups, which has great scientific research and practical significance.

ACKNOWLEDGEMENTS

Thanks to the Shandong Engineering Technology Institute for Groundwater Numerical Simulation and Contamination Control and Shandong Provincial Geo-mineral Engineering Exploration Institute for their technical and data support for this study.

FUNDING

This research was funded by the National Natural Science Foundation of China (41772257) and the innovation team project of colleges and universities in Shandong Province (2018GXRCO12).

DATA AVAILABILITY STATEMENT

All relevant data are included in the paper or its Supplementary Information.

CONFLICT OF INTEREST

The authors declare there is no conflict.

REFERENCES

Agoubi, B. 2021 Review: origin, heating process, and groundwater flow system of non-volcanic thermal aquifers in Tunisia. *Arabian Journal of Geosciences* **14**(5), 369. doi:10.1007/S12517-021-06632-3.

Chi, G. 2019 *Identification of the Dominant Seepage Channel in Jinan Karst Springs*. MA Thesis, University of Jinan, Jinan, China.

Chu, H., Wei, J., Wang, R. & Xin, B. 2017 Characterizing the interaction of groundwater and surface water in the karst aquifer of Fang Shan, Beijing (China). *Hydrogeology Journal* **25**, 575–588. doi:10.1007/s10040-016-1507-7.

Craig, H. 1961 Isotopic variations in meteoric waters. *Science* **133**, 1702–1703. doi:10.1126/science.133.3465.1702.

Dhakate, R. & Singh, V. 2008 Identification of water-bearing fractured zones using electrical conductivity logging in granitic terrain, Andhra Pradesh, India. *Current Science* **95**(8), 1060–1066.

Dong, Y. 2020 *Study on the Hydraulic Characteristics of the Void Structure of Karst Aquifer in Jinan Spring Area*. MA Thesis, University of Jinan, Jinan, China.

Doughty, C., Tsang, C., Yabuuchi, S. & Kunimaru, T. 2013 Flowing fluid electric conductivity logging for a deep artesian well in fractured rock with regional flow. *Journal of Hydrology* **482**, 1–13. doi:10.1016/j.jhydrol.2012.04.061.

Fang, P., Cao, Y., Tang, K., Li, X. & Wang, Z. 1989 Age datings of the ground water in the spring area of Jinan City. *Carsologica Sinica* **8**(01), 49–54. (in Chinese). doi:CNKI:SUN:ZGYR.0.1989-01-007.

Gao, Z., Xu, J., Wang, S., Li, C., Han, K., Li, J., Luo, F. & Ma, H. 2014 The distribution characteristics and hydrogeological significance of trace elements in karst water, Jinan, China. *Earth Science Frontiers* **21**(4), 135–146. (in Chinese). doi:10.13745/j.esf.2014.04.015.

Gao, Z., Zhang, F., An, Y., Xie, W. & Feng, J. 2022 Application of groundwater stratified exploration technology in groundwater flow system research. *Bulletin of Geological Science and Technology* **41**(01), 71–78 + 89. (in Chinese). doi:10.19509/j.cnki.dzkq.2022.0039.

Guo, H. & Wang, Y. 2006 Hydrogeochemistry as an indicator for karst groundwater flow: a case study in the Shantou karst water system, Shanxi, China. *Bulletin of Geological Science and Technology* **25**(03), 85–88. (in Chinese). doi:10.3969/j.issn.1000-7849.2006.03.015.

Hou, G., Zhang, M. & Liu, F. 2008 *Study on Groundwater Exploration in Ordos Basin*. Geological Publishing House, Beijing, China.

Hu, K., Zhang, J. & Xing, L. 2011 Study on dynamic characteristics of groundwater based on the time series analysis method. *Water Sciences and Engineering Technology* (05), 32–34. (in Chinese). doi:10.3969/j.issn.1672-9900.2011.05.012.

Hu, K., Chen, H., Nie, Y. & Wang, K. 2015 Seasonal recharge and mean residence times of soil and epikarst water in a small karst catchment of southwest China. *Scientific Reports* **5**, 10215. doi:10.1038/srep10215.

Jiang, X. 2011 *A Study on Aquifer Systems and Groundwater Flow Systems in Drainage Basins*. PhD Thesis, China University of Geosciences, Beijing, China.

Jiang, G. & Guo, F. 2009 Hydrological character of epikarst in southwest China. *Hydrogeology & Engineering Geology* **36**(05), 89–93. (in Chinese). doi:10.3969/j.issn.1000-3665.2009.05.020.

Jiang, Z. & Yuan, D. 1999 Dynamics features of the epikarst zone and their significance in environments and resources. *Acta Geoscientica Sinica* **20**(03), 302–308. (in Chinese). doi:10.3321/j.issn:1006-3021.1999.03.014.

Khalil, M., Tokunaga, T. & Yousef, A. 2015 Insights from stable isotopes and hydrochemistry to the quaternary groundwater system, South of the Ismailia Canal, Egypt. *Journal of Hydrology* **527**, 555–564. doi:10.1016/j.jhydrol.2015.05.024.

Li, J. 2021 *Study on the Characteristics of Groundwater Flow Systemin the Direct Recharge Area of Baotu Spring Area in Jinan*. MA Thesis, University of Jinan, Jinan, China.

Li, J., Xing, L., Hou, Y., Xing, X., Deng, Z., Zhang, F., Meng, Q. & Wu, D. 2021 Replenishment sources of four great springs in Jinan based on fuzzy similarity priority ratio. *Science Technology and Engineering* **21**(3), 918–926. (in Chinese). doi:10.3969/j.issn.1671-1815.2021.03.011.

Liang, Y. & Zhao, C. 2018 Karst water function in northern China. *China Mining Magazine* **27**(S2), 297–299 + 305. (in Chinese). doi:10.12075/j.issn.1004-4051.2018.S2.078.

Liang, X., Zhang, R., Niu, H., Jin, M. & Sun, R. 2012 Development of the theory and research method of groundwater flow system. *Bulletin of Geological Science and Technology* **31**(05), 143–151. (in Chinese). doi:CNKI:SUN:DZKQ.0.2012-05-020.

Liang, Y., Gao, X., Zhao, C., Tang, C., Shen, H., Wang, Z. & Wang, Y. 2018 Review: characterization, evolution, and environmental issues of karst water systems in northern China. *Hydrogeology Journal* **26**(5), 1371–1385. doi:10.1007/s10040-018-1792-4.

Liang, X., Zhang, R., Luo, M., Sun, R., Jin, M., Zhou, H. & Jiang, L. 2022 Discussion on methodology in research of groundwater flow system: a review of research on groundwater flow systems at CUG-Wuhan. *Bulletin of Geological Science and Technology* **41**(01), 30–42. (in Chinese). doi:10.19509/j.cnki.dzkq.2022.0002.

Liu, Z. 1991 Characteristics of water temperature in epikarst zone and its comparison with that in lower aeration zone. *Carsologica Sinica* **10**(04), 28–33. (in Chinese). doi:CNKI:SUN:ZGYR.0.1991-04-002.

Liu, D., He, P. & Li, Q. 2003 An inverse statistical model for groundwater age in Dabashan tunnel area. *Journal of Railway Engineering Society* **20**(04), 97–101. (in Chinese). doi:10.3969/j.issn.1006-2106.2003.04.024.

Liu, J., Song, X., Yuan, G., Sun, X., Liu, X. & Wang, S. 2010 Characteristics of $\delta^{18}O$ in precipitation over eastern monsoon China and the water vapor sources. *Science Bulletin* **55**(02), 200–211. doi:10.1007/s11434-009-0202-7.

Liu, X., Sun, D., Cao, N., Yuan, N., Huang, H., Tian, C., Zhang, Q., Tang, S., Li, D., Zhou, D. & Dong, F. 2021 Study on the structure of multi-layer water circulation system in the core scenic spot of Huanglong. *Carsologica Sinica* **40**(01), 19–33. (in Chinese). doi:10.11932/karst20210103.

Meng, Q. 2021 *Study on the Differences of the Formation Conditions of the Four Spring Groups in Jinan*. MA thesis, University of Jinan, Jinan, China.

Meng, Q., Wang, X., Xing, L., Dong, Y., Zhu, H., Wu, Z., Li, C., Yu, M. & Hou, Y. 2020 A study of the difference in supply sources of the four groups of springs in Jinan. *Hydrogeology & Engineering Geology* **47**(01), 37–45. (in Chinese). doi:10.16030/j.cnki.issn.1000-3665.201906014.

Phillips, D. & Gregg, P. 2003 Source partitioning using stable isotopes: coping with too many sources. *Oecologia* **136**(2), 261–269. doi:10.1007/s00442-003-1218-3.

Qi, X., Yang, L., Han, Y., Shang, H. & Xing, L. 2012 Cross wavelet analysis of groundwater level regimes and precipitation-groundwater level regime in Ji'nan spring region. *Advances in Earth Science* **27**(09), 969–978. (in Chinese). doi:10.11867/j.issn.1001-8166.2012.09.0969.

Ren, T., Zhao, Q., Chen, B., Gao, P., Chen, J., Deng, G., Kuang, Y., Liu, Y., Wang, W. & Liu, Z. 2000 Tritium concentration and variation of tap water in China. *Chinese Preventive Medicine* (01), 19–21. (in Chinese). doi:CNKI:SUN:ZGYC.0.2000-01-005.

Rose, S. 1993 Environmental tritium systematics of baseflow in piedmont province watersheds, Georgia (USA). *Journal of Hydrology* **143**(3-4), 191–216. doi:10.1016/0022-1694(93)90192-C.

Sappa, G., Barbieri, M., Ergul, S. & Ferranti, F. 2012 Hydrogeological conceptual model of groundwater from carbonate aquifers using environmental isotopes (^{18}O, ^{2}H) and chemical tracers: a case study in Southern Latium Region, Central Italy. *Journal of Water Resource and Protection* **4**(9), 695–716. doi:10.4236/jwarp.2012.49080.

Selene, O., Oscar, E., Jürgen, M., Lucia, O., Yuri, T., Dante, J., Olivia, Z. & Javier, T. 2020 Water-rock interaction and mixing processes of complex urban groundwater flow system subject to intensive exploitation: the case of Mexico City-ScienceDirect. *Journal of South American Earth Sciences* **103**, 102719. doi:10.1016/j.jsames.2020.102719.

Sun, B. & Peng, Y. 2014 Boundary condition, water cycle and water environment changes in the Jinan spring region. *Carsologica Sinica* **33**(03), 272–279. (in Chinese).

Sun, B., Xu, J., Peng, Y. & Lin, G. 2017 Coordination assessment of urban construction and ecological environment protection of spring in Jinan. *Yellow River* **39**(06), 77–81. (in Chinese). doi:10.3969/j.issn.1000-1379.2017.06.017.

Sun, B., Xing, L., Peng, Y. & Li, C. 2021 Characteristics, formation models and water cycle differences of ten major spring groups in Jinan City. *Carsologica Sinica* **40**(03), 409–419. (in Chinese). doi:10.11932/karst20210301.

Toth, J. 1963 A theoretical analysis of groundwater flow in small drainage basins. *Journal of Geophysical Research* **68**(16), 4795–4812. doi:10.1029/JZ068i016p04795.

Wang, J. 2015 *A Methodological Study on the Identification of Hierarchically Nested Groundwater Flow Systems in Drainage Basins*. PhD Thesis, China University of Geosciences, Beijing, China.

Wang, J. 2016 *Analysis and Identification of Hierarchical Groundwater Flow System in Jinan*. PhD Thesis, China University of Geosciences, Beijing, China.

Wang, Z., Liang, Y., Tang, C., Shen, H., Zhao, C., Guo, F., Xie, H. & Zhao, Y. 2020 Ecological restoration pattern and quantitative evaluation of recirculation measures for northern discontinuous karst spring: a case study of Jinci spring in Taiyuan City, Shanxi Province. *Geology in China* **47**(06), 1726–1738. (in Chinese). doi:10.12029/gc20200610.

Wang, J., Liang, X., Ma, B., Liu, Y., Jin, M., Knappett, S. & Liu, Y. 2021 Using isotopes and hydrogeochemistry to characterize groundwater flow systems within intensively pumped aquifers in an arid inland basin, northwest China. *Journal of Hydrology* **595**, 126048. doi:10.1016/J.JHYDROL.2021.126048.

Xiao, W., Sun, R., Chen, M. & Yang, Y. 2022 Interaction between seepage and temperature fields in different groundwater flow systems. *Bulletin of Geological Science and Technology* **41**(01), 251–259. (in Chinese). doi:10.19509/j.cnki.dzkq.2022.0032.

Xing, L. 2006 Protection of karst water environment in Ji'nan spring's region. *Water Conservancy Science and Technology and Economy* **12**(09), 601–604. (in Chinese). doi:10.3969/j.issn.1006-7175.2006.09.013.

Xing, L., Wu, Q., Ye, C. & Ye, N. 2010 Groundwater environmental capacity and Its evaluation index. *Environmental Monitoring and Assessment* **169**(1-4), 217–227. doi:10.1007/s10661-009-1163-7.

Xing, L., Zhou, J., Song, G. & Xing, X. 2018 Mixing ratios of recharging water sources for the four largest spring groups in Jinan. *Earth Science Frontiers* **25**(3), 260–272. (in Chinese). doi:10.13745/j.esf.2018.03.021.

Yang, X. 2008 *Estimation of Groundwater Recharge and Renewal Rate Based on Environmental Isopes in Songnen Plain*. PhD Thesis, China University of Geosciences, Beijing, China.

Yang, L., Liu, C. & Qi, X. 2016 Study on characteristic variation of hydro-chemistry of Jinan spring. *Journal of Water Resources and Water Engineering* **27**(1), 59–64. (in Chinese). doi:10.11705/j.issn.1672-643X.2016.01.10.

Yuan, D. 2010 The situation and tasks for northern karst research of our country. *Carsologica Sinica* **29**(03), 219–221. (in Chinese). doi:CNKI:SUN:ZGYR.0.2010-03-002.

Zhang, R., Liang, X., Jin, M., Wan, L. & Yu, Q. 2012 *Fundamentals of Hydrogeology*. Geological Publishing House, Beijing, China.

First received 9 April 2022; accepted in revised form 29 June 2022. Available online 7 July 2022